

Modelling the Effect of Multiaxial Stress on Magnetic Hysteresis of Electrical Steel Sheets: A Comparison

U. Aydin¹, P. Rasilo^{1,2}, F. Martin¹, D. Singh¹, L. Daniel³, A. Belahcen¹, R. Kouhia⁴ and A. Arkkio¹

¹Department of Electrical Engineering and Automation, Aalto University, Espoo, Finland

²Department of Electrical Engineering, Tampere University of Technology, Tampere, Finland

³Group of Electrical Engineering-Paris, CNRS(UMR 507)/Supélec/UPMC/Univ Paris-Sud, Gif-sur-Yvette F-91192, France

⁴Department of Mechanical Engineering and Industrial Systems, Tampere University of Technology, Tampere, Finland

The abilities of a simplified multiscale and a Helmholtz energy based models from literature to predict the multiaxial stress dependent magnetic hysteresis behavior of electrical steel sheets are analyzed. The identification of the models are performed using only uniaxial magneto-mechanical measurements. Reasonable accuracy between the measurements and the modeled results are obtained. With this study, the applicability of the Helmholtz energy based model for predicting the multiaxial magneto-mechanical behavior of electrical steel sheets is verified for the first time. The differences between the studied models and possible modifications to increase the accuracy of them are discussed. Some brief guidelines for the applications are given.

Index Terms—Magnetic hysteresis, magneto-mechanical effects, multiaxial stress, multiscale modeling.

I. INTRODUCTION

Magnetic properties of the ferromagnetic materials are known to be stress dependent [1], [2]. In most practical applications, where ferromagnetic materials are widely used, material is subject to multi-axial stresses which are arising during their operation or due to manufacturing processes [2]-[4]. Several studies have shown that these magneto-mechanical loadings have significant effects on the performance of rotating electrical machines [4], [5]. Therefore, in order to accurately analyze the existing devices and design more efficient ones, characterization of ferromagnetic materials under multiaxial magneto-mechanical loadings are required.

Earlier several studies were performed to model the anhysteretic magneto-mechanical behavior of electrical steel sheets under multiaxial loadings [5]-[9]. For instance, in [5] and [6] the multiaxial modeling is performed with uniaxial models using an equivalent stress concept. Although this modeling approach can be successful for a particular biaxial configuration, it can be highly inaccurate for some cases [6]. In [9] a multiscale approach is adopted by defining a local free energy at the domain scale and obtaining macroscopic magneto-elastic behavior by homogenization of local behavior. In [10] the magnetic hysteresis is included to multiscale model by taking into account the dissipation phenomenon using the approach from [11]. Although this multiscale model is able to model the multiaxial magneto-elastic behavior successfully it is computationally too heavy to be implemented in numerical tools. In order to reduce the computation time and keep benefit from the multiscale approach potentialities, a simplified version of the multiscale

model including magnetic hysteresis is developed in [12]. On the other hand, in [8] a Helmholtz free energy density is defined as a function of five scalar invariants of the magneto-mechanical loading and the anhysteretic material behavior is obtained by minimizing this energy. In [13] the anhysteretic Helmholtz energy based model is extended to account for the magnetic hysteresis by implementing the model into Jiles-Atherton (JA) hysteresis model [14] and it was shown to be successful under uniaxial magneto-mechanical loadings.

Objective of this paper is to investigate the possibility of using simplified multiscale (SM) and Helmholtz energy based (HE) models, which are suitable to be used in numerical tools, from [12] and [13] for the prediction of multiaxial stress dependent magnetic hysteresis when only uniaxial measurements are available. The modelling parameters of the models are identified for non-oriented electrical steel sheet using only uniaxial magneto-mechanical measurements. The modeled hysteresis loops, hysteresis losses and coercive fields under multiaxial magneto-mechanical loadings are compared to measured data. Advantages and disadvantages of the models are discussed and brief guidelines are given.

II. MAGNETO-MECHANICAL MODELS

A. Simplified Multiscale (SM) Model

In the SM model the material is modeled as a single crystal that consists of randomly oriented magnetic domains. Considering isotropic material, the local potential energy W_k of a domain is expressed as the sum of magneto-static energy W_k^{mag} and magneto-elastic energy W_k^{me} , and it is given by

$$W_k = W_k^{\text{mag}} + W_k^{\text{me}} = -\mu_0 \mathbf{H} \cdot \mathbf{M}_k - \boldsymbol{\sigma} : \boldsymbol{\epsilon}_k^{\mu} \quad (1)$$

where μ_0 is permeability of free space, \mathbf{H} and $\boldsymbol{\sigma}$ are the applied magnetic field strength and mechanical stress, whereas \mathbf{M}_k and $\boldsymbol{\epsilon}_k^{\mu}$ are the local magnetization and magnetostriction strain, respectively. Local magnetization \mathbf{M}_k and magnetostriction strain $\boldsymbol{\epsilon}_k^{\mu}$, for a domain oriented along \mathbf{u}_k , are

Manuscript received Xxxxxxxx xx, xxxx; revised Xxxxxxxx xx, xxxx; accepted Xxxxxxxx xx, xxxx. Date of publication Xxxx xx, xxxx; date of current version Xxxxxxxx xx, xxxx. Corresponding author: U. Aydin. (e-mail: ugur.aydin@aalto.fi).

Color versions of one or more of the figures in this paper are available online at <http://ieeexplore.ieee.org>.

Digital Object Identifier (inserted by IEEE).

classically given as

$$\mathbf{M}_k = M_s \mathbf{u}_k = M_s [\tau_1 \ \tau_2 \ \tau_3]^T \quad (2)$$

$$\boldsymbol{\varepsilon}_k^\mu = \lambda_s \left(\frac{3}{2} \mathbf{u}_k \otimes \mathbf{u}_k - \frac{1}{2} \mathbf{I} \right) \quad (3)$$

where M_s and λ_s are the magnetization and macroscopic magnetostriction of the saturated material, respectively. \mathbf{I} is the second order identity tensor and τ_1, τ_2, τ_3 are the direction cosines of the magnetization orientation vector \mathbf{u}_k . The volume fraction f_k of a given set of domains with magnetization orientation \mathbf{u}_k is calculated by using a Boltzmann probability function

$$f_k = \frac{\exp(-A_s W_k)}{\int_k \exp(-A_s W_k)} \quad (4)$$

where A_s is a material parameter that is a function of unstressed anhysteretic initial susceptibility χ_0 and is given by $A_s = 3\chi_0 / \mu_0 M_s$.

Using the defined volume fraction and an integration operation over all possible magnetization directions \mathbf{u}_k , the macroscopic magnetization \mathbf{M} and magnetostriction $\boldsymbol{\varepsilon}^\mu$ are obtained as the volume average of the corresponding local quantities:

$$\mathbf{M} = \langle \mathbf{M}_k \rangle = \int_k f_k \mathbf{M}_k \quad \text{and} \quad \boldsymbol{\varepsilon}^\mu = \langle \boldsymbol{\varepsilon}_k^\mu \rangle = \int_k f_k \boldsymbol{\varepsilon}_k^\mu \quad (5)$$

These integrations are computed numerically by discretization of a unit sphere for the possible orientations \mathbf{u}_k .

So far, the presented model is anhysteretic. The magnetic hysteresis is implemented to the model by adding an irreversible magnetic field contribution \mathbf{H}_{irr} whose definition is based on [11]. The implementation of \mathbf{H}_{irr} to SM model is detailed in [12] and it will be repeated here briefly. Assuming \mathbf{H}_{irr} is parallel to \mathbf{H} , the norm of \mathbf{H}_{irr} is given as

$$\|\mathbf{H}_{\text{irr}}\| = \delta \left(\frac{k_r}{\mu_0 M_s} + c_r \|\mathbf{H}\| \right) \times \left(1 - \kappa \exp\left(\frac{k_a}{\kappa} \|\mathbf{M} - \mathbf{M}_{\text{inv}}\| \right) \right) \quad (6)$$

where $\delta = 1$ initially, and the sign of it changes on each inversion of magnetic loading direction. k_r, c_r, k_a , and κ are material parameters. The initial value of κ is κ_0 which is a material constant. The value of κ is a function of its previous value κ_0 and it changes its value each time there is a change in the loading direction. The function for κ is given as

$$\kappa = 2 - \kappa_0 \exp\left(-\frac{k_a}{\kappa_0} \|\mathbf{M} - \mathbf{M}_{\text{inv}}\| \right) \quad (7)$$

where \mathbf{M}_{inv} is the value of \mathbf{M} at the previous inversion of loading direction. The stress dependent coercive field is modeled with k_r that is given as

$$k_r = k_r^0 \left(1 - \zeta \left(N_\sigma - \frac{1}{3} \right) \right) \quad (8)$$

where k_r^0 is a material constant and ζ being an adjustment parameter. The function N_σ is a stress-demagnetisation factor given by [12]

$$N_\sigma = \frac{1}{1 + 2 \exp(-3A_s \lambda_s \sigma_{\text{eq}} / 2)} \quad (9)$$

$$\sigma_{\text{eq}} = \frac{3}{2} \mathbf{h} \cdot \left(\boldsymbol{\sigma} - \frac{1}{3} \text{tr}(\boldsymbol{\sigma}) \mathbf{I} \right) \cdot \mathbf{h} \quad (10)$$

Here σ_{eq} is an equivalent stress defined as the projection of the deviatoric part of $\boldsymbol{\sigma}$ along the magnetic field direction \mathbf{h} [6]. The parameters c_r and k_a have constant values. The identification procedure for the material parameters are given in Section III. After the calculation of \mathbf{H}_{irr} the effective field is then obtained as

$$\mathbf{H}_{\text{eff}} = \mathbf{H} + \mathbf{H}_{\text{irr}} \quad (11)$$

A configuration field can also be added to \mathbf{H}_{eff} in order to consider the non-monotonic effect of stress on magnetic permeability [12]. In this work it is neglected since it did not affect the accuracy of the model for the studied material.

B. Helmholtz Energy Based (HE) Model

The model is detailed in [13] and will be summarized here. In this model anhysteretic magneto-mechanical behavior of material is obtained from a Helmholtz free energy density ψ [8], [13]. Assuming an isotropic material ψ is expressed as a function of five scalar invariants which depend on magnetic flux density vector \mathbf{B} and total strain tensor $\boldsymbol{\varepsilon}$:

$$\begin{aligned} I_1 &= \text{tr}(\boldsymbol{\varepsilon}), \quad I_2 = \frac{1}{2} \text{tr}(\boldsymbol{\varepsilon}^2), \quad I_3 = \det(\boldsymbol{\varepsilon}) \\ I_4 &= \frac{\mathbf{B} \cdot \mathbf{B}}{B_{\text{ref}}^2}, \quad I_5 = \frac{\mathbf{B} \cdot (\tilde{\boldsymbol{\varepsilon}} \mathbf{B})}{B_{\text{ref}}^2}, \quad I_6 = \frac{\mathbf{B} \cdot (\tilde{\boldsymbol{\varepsilon}}^2 \mathbf{B})}{B_{\text{ref}}^2} \end{aligned} \quad (12)$$

where $B_{\text{ref}} = 1$ T. The first three invariants describe purely mechanical loading. The fourth invariant I_4 is chosen to describe the single-valued magnetization behavior, whereas I_5 and I_6 describe the magneto-elastic coupling, and they are written using deviatoric part of the strain $\tilde{\boldsymbol{\varepsilon}}$. The expression for the Helmholtz free energy density is then given as

$$\psi = \frac{1}{2} \lambda I_1^2 + 2G I_2 - \nu_0 \left(\frac{I_4}{2} + \sum_{i=0}^{n_a-1} \frac{\alpha_i}{i+1} I_4^{i+1} + \sum_{i=0}^{n_\beta-1} \frac{\beta_i}{i+1} I_5^{i+1} + \sum_{i=0}^{n_\gamma-1} \frac{\gamma_i}{i+1} I_6^{i+1} \right) \quad (13)$$

Here λ and G are the Lamé constants of the material, ν_0 is the reluctivity of free space and $\alpha_i, \beta_i, \gamma_i$ are the fitting parameters to be identified from measurements. The magnetization and magneto-elastic stress are obtained as

$$\boldsymbol{\sigma}_{me}(\mathbf{B}, \boldsymbol{\varepsilon}) = \frac{\partial \psi(\mathbf{B}, \boldsymbol{\varepsilon})}{\partial \boldsymbol{\varepsilon}} \quad \text{and} \quad \mathbf{M}(\mathbf{B}, \boldsymbol{\varepsilon}) = -\frac{\partial \psi(\mathbf{B}, \boldsymbol{\varepsilon})}{\partial \mathbf{B}} \quad (14)$$

Next, the presented anhysteretic model is implemented to JA hysteresis model [14]. Following five equations summarize the model.

$$\mathbf{H}_{\text{eff}} = \mathbf{H} + \alpha \mathbf{M} \quad (15)$$

$$\mathbf{M}_{\text{an}} = \mathbf{F}(\mathbf{H}_{\text{eff}}) \quad (16)$$

$$\mathbf{d} = \mathbf{M}_{\text{an}} - \mathbf{M}_{\text{irr}} \text{ and } \delta = \frac{d\mathbf{B}}{dt} \cdot \mathbf{d} \quad (17)$$

$$\frac{d\mathbf{M}_{\text{irr}}}{d\mathbf{H}_{\text{eff}}} = \begin{cases} \mathbf{k}(\tilde{\boldsymbol{\varepsilon}})^{-1} \frac{d\mathbf{d}^T}{|\mathbf{d}|}, & \text{if } |\mathbf{d}| > 0 \text{ and } \delta > 0 \\ 0, & \text{otherwise} \end{cases} \quad (18)$$

$$\frac{d\mathbf{M}}{d\mathbf{H}_{\text{eff}}} = c \frac{d\mathbf{M}_{\text{an}}}{d\mathbf{H}_{\text{eff}}} + (1-c) \frac{d\mathbf{M}_{\text{irr}}}{d\mathbf{H}_{\text{eff}}} \quad (19)$$

where α and c are constant parameters to be identified. Equation (17) is replaced by the anhysteretic model obtained from HE model. The details of this implementation can be found in [13]. The stress dependency of coercive field is introduced by pinning parameter \mathbf{k} that is an isotropic function of deviatoric strain. It is given by

$$\mathbf{k}(\tilde{\boldsymbol{\varepsilon}}) = k_0 (\mathbf{I} + a\tilde{\boldsymbol{\varepsilon}} + b\tilde{\boldsymbol{\varepsilon}}^2) \quad (20)$$

where the parameters k_0 , a , and b are constants and their values will be determined from measurements.

III. IDENTIFICATION OF MODELS

The model parameters are identified for a grade M330-50A 3% Fe-Si non-oriented electrical steel sheet. For the identification purpose uniaxial magneto-mechanical measurement data from [2] is used. In the experiment process a cross-shaped sample was magnetized along rolling direction (x) and loaded by stresses varying from 100 MPa compression (-) to 100 MPa tension (+) including biaxial ones. The surface magnetic field strength and the magnetic flux density were measured at 50 Hz using H -coils and needle probes, respectively.

To model the anhysteretic behavior by SM model three physical based parameters M_s , λ_s and A_s are required to be identified. The parameters M_s and A_s are identified from single anhysteretic measurement under no applied stress. Saturation magnetostriction λ_s can be identified from a single magnetostriction curve under zero stress and high applied field that saturates the material. Since there was no magnetostriction measurements available this parameter is approximated for 3% Fe-Si alloy from [15]. In order to describe the hysteresis, parameters k_r^0 , τ , c_r , κ_0 and k_a are also needed to be identified. These parameters are determined by least-squares fitting to a measured major hysteresis loop under no applied stress. The determined SM model parameters are $M_s = 1.28$ MA/m, $\lambda_s = 7 \cdot 10^{-6}$, $\chi_0 = 2300$, $k_r^0 = 150$ J/m³, $c_r = 0.01$, $k_a = 20.7 \cdot 10^{-6}$ m/A, $\kappa_0 = 0.012$, $\zeta = 0.35$.

On the other hand, to describe the anhysteretic magneto-mechanical behavior with HE model, parameters α_i , β_i , γ_i are needed to be identified. The parameters are identified by least squares fitting of modeling results to the four measured anhysteretic curves under uniaxial stresses of -50 MPa, 0 MPa, 25 MPa and 100 MPa which are applied parallel to magnetic field. The two curves under low and high tensile are chosen

for the identification in order to take into account possible non-monotonic effect of tensile stress on permeability as seen in [13]. It is worth mentioning that, the number of fitting parameters, n_α , n_β , and n_γ for the HE model is material dependent. Afterwards, in order to model the magnetic hysteresis, parameters α , c , k_0 , a , and b are fitted by least-squares comparison of the modeled major hysteresis loops to the measured ones under aforementioned mechanical stresses. The determined HE model parameters are $\lambda = 145$ GPa, $G = 68.3$ GPa, $n_\alpha = 8$, $n_\beta = 1$, $n_\gamma = 1$, $\alpha_0, \dots, \alpha_7 = 242.30, 60.98, -148.70, 643.45, -993.5, 740.81, -261.72, 365.04$ J/m³, $\beta_0 = -0.54$ J/m³, and $\gamma_0 = 372.50$ J/m³, $\alpha = 7.97 \cdot 10^{-5}$, $c = 0.0125$, $k_0 = 113.04$ A/m, $a = -142$, and $b = 4.81 \cdot 10^{-5}$.

IV. RESULTS

The modeled hysteresis loops by both models under several stress states are compared to measurements in Fig. 1. Here, applied stress is given with notation $\boldsymbol{\sigma} = [\sigma_x \sigma_y]$, where y represents the transverse direction. Other components of the applied stress tensor are kept zero [2]. Predicted hysteresis loops by both models show reasonable accuracy compared to measured ones.

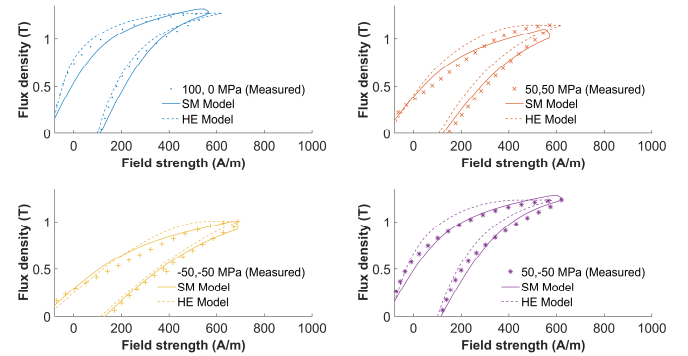


Fig. 1. Comparison of the experimental and the modeled hysteresis loops under several stress states.

In Fig. 2(a) measured stress dependent hysteresis losses are shown. In Fig. 2(b) and 2(c) relative errors between the measured hysteresis losses and the modeled results from SM and HE models are given, respectively. Both models predict the losses consistently under studied stress range. Relative errors between the measured and modeled losses vary between -25.9% to 13.6% for the SM model and -8.6% to 9.3% for the HE model. The highest error for the SM model is observed under pure shear case when the applied stress is higher than 75 MPa. For the HE model, error is the highest when high level of uniaxial stress is applied in the transverse direction.

The measured coercive field evolution under stress is shown in Fig. 3(a). Relative errors between the measurements and modelling results obtained from SM and HE models are presented in Fig. 3(b) and 3(c), respectively. Both models are successful catching the behavior with acceptable accuracy with relative errors varying between 5.4% to -31.6% for SM model and -1.8% to -35.3% for HE model compared to measurements. The highest errors are observed under the conditions where the highest hysteresis loss errors are present.

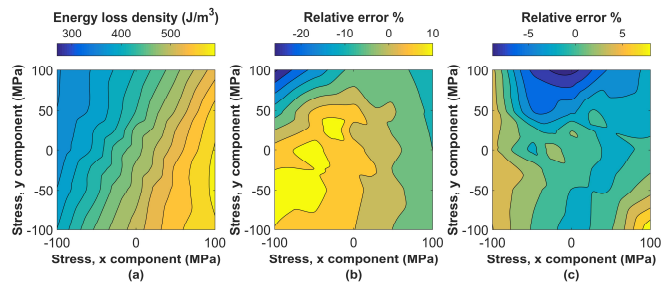


Fig. 2. (a) Measured hysteresis losses. (b) Errors between measurements and SM model results. (c) Errors between measurements and HE model results.

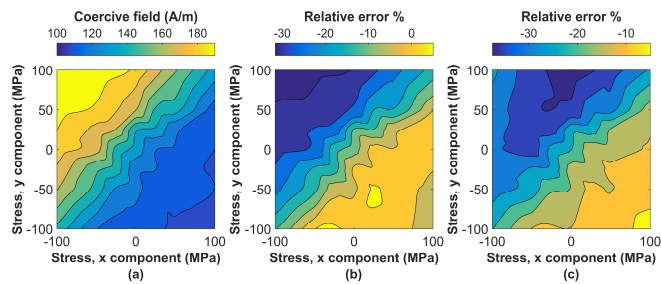


Fig. 3. (a) Measured coercive fields. (b) Errors between measurements and SM model results. (c) Errors between measurements and HE model results.

V. DISCUSSION AND CONCLUSION

Two magneto-mechanical models from literature to predict the multiaxial stress dependency of magnetic hysteresis were studied. The models were identified from uniaxial measurements and it has been shown by comparing to measured data that they can predict the magnetic hysteresis under multiaxial stresses with acceptable accuracy, considering the simplicity of the models. By this comparison we also have verified for the first time that the HE model is able to predict the multiaxial magneto-mechanical behavior of electrical steel sheets with reasonable accuracy.

Considering the identification of the models, SM model requires only one stress free anhysteretic curve and hysteresis loop measurements to be identified whereas, HE model requires several measurements under uniaxial stress. Therefore, if measurements under stress are not available SM model is favorable. On the other hand, in order to be able to implement the presented SM model with hysteresis to the numerical tools, such as finite element analysis, one needs to vectorize the hysteresis model of it. Hysteresis HE model on the other hand, can directly be implemented to such numerical tools. Moreover, since its input variables are \mathbf{B} and $\boldsymbol{\varepsilon}$, it is easier to implement to general vector potential and displacement field formulations. For instance, if stress dependent measurements are not available, SM model can be used to provide stress dependent data for identifying the HE model which then can be used in numerical computations.

Accuracy of the SM model can be improved by replacing (10) with another equivalent stress definition which might help improving the accuracy of stress dependent coercive field calculation. Another approach could be to introduce stress dependent saturation magnetostriction coefficient if magnetostriction measurements under stress are available.

This might help obtaining closer anhysteretic curves to the measured ones resulting more accurate hysteresis loops modelling. More accurate stress dependent coercive field can be obtained from HE model for instance, by making the parameter k_0 stress dependent. For the anhysteretic part, higher accuracy can be obtained by increasing the number of material parameters n_α , n_β , and n_γ with the expense of slower computation. Also, if available using magnetization curves under multiaxial loading during identification would increase the accuracy of this model. Modifications to the models are currently under study and will be part of a future work.

ACKNOWLEDGMENT

The research leading to these results has received funding from the European Research Council under the European Union's Seventh Framework Programme (FP7/2007-2013) / ERC grant agreement n°339380. The Academy of Finland is acknowledged for financial support.

REFERENCES

- [1] R.M. Bozorth, *Ferromagnetism*. pp. 595–712. Van Nostrand Company, New York (1951).
- [2] M. Rekik, O. Hubert, and L. Daniel, "Influence of a Multiaxial Stress on the Reversible and Irreversible Magnetic Behaviour of 3% Si-Fe Alloy," *Int. J. Appl. Electromagn. Mech.*, vol. 44, no. 3-4, pp. 301-315, 2014.
- [3] P. Baudouin, A. Belhadj, F. Breaban, A. Deffontaine, and Y. Houbaert, "Effects of Laser and Mechanical Cutting Modes on the Magnetic Properties of Low and Medium Si Content Nonoriented Electrical Steels," *IEEE Trans. on Magn.*, vol. 38, no. 5, pp. 3213-3215, 2002.
- [4] S. Zeze, Y. Kai, T. Todaka, and M. Enokizono, "Vector Magnetic Characteristic Analysis of a PM Motor Considering Residual Stress Distribution with Complex-Approximated Material Modelling," *IEEE Trans. Magn.*, vol. 48, no. 11, pp. 3352-3355, 2012.
- [5] K. Yamazaki, and Y. Kato, "Iron Loss Analysis of Interior Permanent Magnet Synchronous Motors by Considering Mechanical Stress and Deformation of Stators and Rotors," *IEEE Trans. Magn.*, vol. 50, no. 2, pp. 7022504, 2014.
- [6] O. Hubert, L. Daniel, "Energetic and multiscale approaches for the definition of an equivalent stress for magneto-elastic couplings", *J. Magn. Mater.*, vol. 323, iss. 13, pp. 1766-1781, 2011.
- [7] H. Ebrahimi, Y. Gao, H. Dozono, and K. Muramatsu, "Coupled Magneto-Mechanical Analysis in Isotropic Materials Under Multiaxial Stress," *IEEE Trans. Magn.*, vol. 50, no. 2 pp. 7006904, 2014.
- [8] K. A. Fonteyn, A. Belahcen, R. Kouhia, P. Rasilo, and A. Arkkio, "FEM for Directly Coupled Magneto-Mechanical Phenomena in Electrical Machines," *IEEE Trans. Magn.*, vol. 46, no. 8, pp. 2923-2926, 2010.
- [9] L. Daniel, O. Hubert, N. Buiron, R. Billardon, "Reversible magneto-elastic behavior: a multiscale approach", *J. Mech. Phys. Sol.*, vol. 56, pp. 1018-1042, 2008.
- [10] L. Daniel, M. Rekik, O. Hubert, "A Multiscale Model for Magneto-Elastic Behaviour Including Hysteresis Effects," *Arch. Appl. Mech.*, vol. 84, issue 9, pp. 1307-1323, 2014.
- [11] Hauser, H. "Energetic model of ferromagnetic hysteresis: Isotropic magnetization". *J. Appl. Phys.* vol. 96, no. 5, pp. 2753-2767, 2004.
- [12] L. Daniel, O. Hubert, and M. Rekik, "A Simplified 3-D Constitutive Law for Magnetomechanical Behavior," *IEEE Trans. Magn.*, vol. 51, no. 3, 2015.
- [13] P. Rasilo et al., "Modeling of hysteresis losses in ferromagnetic laminations under mechanical stress," *IEEE Trans. Magn.*, vol. 52, no. 3, pp. 7300204, 2016.
- [14] D. C. Jiles, J. B. Thielke, M. K. Devine, "Numerical Determination of Hysteresis Parameters for the Modeling of Magnetic Properties Using the Theory of Ferromagnetic Hysteresis", *IEEE Trans. Magn.*, vol. 28, no. 1, 1992.
- [15] L. Daniel, O. Hubert, R. Billardon, "Homogenisation of magneto-elastic behaviour : from the grain to the macro scale", *Comp. App. Math.*, vol. 23, no. 2-3, pp. 285-308, 2004.